

# Bivariate temporal dependence via mixtures of rotated copulas

RUYI PAN, LUIS E. NIETO-BARAJAS, RADU CRAIU

*University of Toronto & ITAM*

ruyi.pan@mail.utoronto.ca, luis.nieto@itam.mx & radu.craiu@utoronto.ca

## Abstract

Parametric bivariate copula families have been known to flexibly capture enough various dependence patterns, e.g., either positive or negative dependence in either the lower or upper tails of bivariate distributions. However, to the best of our knowledge, there is not a single parametric model adaptable enough to capture several of these features simultaneously. To address this, we propose a mixture of 4-way rotations of a parametric copula that is able to capture all these features. We illustrate the construction using the Clayton family but the concept is general and can be applied to other families. In order to include dynamic dependence regimes, the approach is extended to a time-dependent sequence of mixture copulas in which the mixture probabilities are allowed to evolve in time via a moving average type of relationship. The properties of the proposed model and its performance are examined using simulated and real data sets.

*Keywords:* Bayesian inference, copulas, dependence models, mixtures, moving average process, time varying copulas.

## 1 Introduction

Copulas have emerged in recent years as viable tools for modeling dependence in non-standard situations in which the usual "suspects" such as multivariate Gaussian, Student or Wishart distributions are not appropriate. Besides having a methodological contender with an equal potential for applications, copulas have been lauded in the literature for possessing several features that are desirable to a statistician. Allowing the separation of modeling

effort for the marginal models and the dependence structure continues to rank high, but so is the flexibility it exhibits in capturing dependence patterns using parametric families, especially for bivariate data. In higher dimensions this flexibility is expressed through the use of C- or D- vine copulas [2]. However, while one can identify copula families able to capture a bivariate distribution's various patterns of lower or upper tail dependence, be they positive or negative, we do not know of any parametric family that can capture several such patterns *simultaneously*.

This paper aims to close this gap in the copula literature by considering mixtures of rotating copulas which are able to capture similar dependence in all tail regions of the unit square. Mixture of copulas have been used previously in the literature to model the dependence between successive states in a Markov chain [7] or to model dependence using a mixture of tree-copulas in which each component is assumed to be a Markov distribution with respect to a tree with a given edge set [11]. Our model is distinct in its inception and motivation.

In the analysis of extreme value data, it is often desirable to measure the tail dependence in a bivariate vector. Some copulas are able to capture tail dependence, for instance the Clayton copula with positive  $\theta$  parameter exhibits upper (right) tail dependence [8].

In this paper we first generalise the concept of bivariate tail dependence to the four corners of the unit square and propose a flexible copula that is able to capture any type of tail dependence. Our goal is achieved by mixing 4 rotated instances of the Clayton copula, to 0, 90, 180 and 270 degrees. Furthermore, the 4-dimensional mixture weights  $\pi$  are allowed to change over time,  $\pi_t$ , through a moving average type of process of order  $q$  that maintains the marginal distribution invariant over time.

The contents of the rest of the paper is as follows. In Section 2 we provide the motivation of the paper and the required notation. Section 3 contains the four-way tail dependence and show that the Clayton rotations measure the four types of tail dependence. In Section 4 we

define our mixture model for a specific time and define the time dependent mixture weights and Section 5 provides a Bayesian analysis of the model and an illustration of its performance is reported in Section 6. Section 7 contains conclusions and directions for future work.

## 2 Motivation and Notation

The emergence of copulas as important tools for modeling dependence has its origins in Sklar’s paper [12] which demonstrated that the link between any continuous multivariate distribution and its marginals can be completed via a unique copula  $C : [0, 1]^m \rightarrow [0, 1]$ . The latter is a multivariate distribution with uniform marginals on the interval  $[0, 1]$ . Specifically, if  $F$  is a multivariate cumulative distribution function (CDF) with marginal CDFs  $F_1, \dots, F_m$  then  $F(x_1, \dots, x_m) = C\{F_1(x_1), \dots, F_m(x_m)\}$ . Additionally, the copula function can be obtained as  $C(u_1, \dots, u_m) = F\{F_1^{-1}(u_1), \dots, F_m^{-1}(u_m)\}$ , where  $F_j^{-1}$  for  $j = 1, \dots, m$  are the marginal inverse CDFs or quantile functions.

There is a vast body of literature devoted to identifying parametric copula families that are able to capture various dependence patterns in the tails [5]. For instance, in the analysis of extreme value theory an important concept is that of dependence in the upper-right or lower-down quadrants of a joint bivariate distribution. This is quantified by the so-called upper and lower tail dependence coefficients [3, 5].

Let  $(X_1, X_2)$  be a bivariate vector with marginal CDFs  $F_1$  and  $F_2$  such that the joint CDF is given in terms of the copula  $C$  as  $F(x_1, x_2) = C(F_1(x_1), F_2(x_2))$ . Tail dependence coefficients are defined as the conditional probabilities that both variables are above an upper quantile of order  $1 - \nu$ , or both variables are below a lower quantile of order  $\nu$ . We denote

$$\lambda_{UU} = \lim_{\nu \rightarrow 0} P\{X_1 > F_1^{-1}(1 - \nu) \mid X_2 > F_2^{-1}(1 - \nu)\}$$

for the upper-right (upper-upper) corner, and

$$\lambda_{LL} = \lim_{\nu \rightarrow 0} P\{X_1 \leq F_1^{-1}(\nu) \mid X_2 \leq F_2^{-1}(\nu)\}$$

for the lower-down (lower-lower) corner, where sub indexes  $U$  and  $L$  mean upper and lower, respectively. However it is possible that both variables have comovements in the opposite tails, that is, one variable has values in the upper quantile and the other in the lower quantile, or conversely. In this case the opposite tail dependence is defined as

$$\lambda_{UL} = \lim_{\nu \rightarrow 0} \text{P}\{X_1 > F_1^{-1}(1 - \nu) \mid X_2 \leq F_2^{-1}(\nu)\}$$

for the upper-lower corner, and

$$\lambda_{LU} = \lim_{\nu \rightarrow 0} \text{P}\{X_1 \leq F_1^{-1}(\nu) \mid X_2 > F_2^{-1}(1 - \nu)\}$$

for the lower-upper corner.

These four tail dependence coefficients can be written entirely in terms of the copula. It is straightforward to show that

$$\begin{aligned} \lambda_{UU} &= \lim_{\nu \rightarrow 0} \frac{2\nu - 1 + C(1 - \nu, 1 - \nu)}{\nu}, & \lambda_{LL} &= \lim_{\nu \rightarrow 0} \frac{C(\nu, \nu)}{\nu}, \\ \lambda_{UL} &= \lim_{\nu \rightarrow 0} \frac{\nu - C(1 - \nu, \nu)}{\nu}, & \lambda_{LU} &= \lim_{\nu \rightarrow 0} \frac{\nu - C(\nu, 1 - \nu)}{\nu}. \end{aligned} \quad (1)$$

It is well known [e.g. 16] that the Clayton copula exhibits lower-lower tail dependence, whereas the Gumbel copula has upper-upper tail dependence. One way of defining copulas with the four types of tail dependence (1) is by means of rotation as in [6]. It is easy to see from (1) that for most copulas, the four tail dependence coefficients will be different. In the next section, we develop a mixture of copulas that allows identical tails dependence coefficients.

Before we proceed let us introduce some notation.  $\text{Ga}(\alpha, \beta)$  denotes a gamma density with mean  $\alpha/\beta$ ;  $\text{Be}(\alpha, \beta)$  denotes a beta density with mean  $\alpha/(\alpha + \beta)$ ;  $\text{Dir}(\boldsymbol{\alpha})$  denotes a Dirichlet density with parameter vector  $\boldsymbol{\alpha}$ ;  $\text{Mult}(c, \mathbf{p})$  denotes a multinomial density with total trials  $c$  and probability vector  $\mathbf{p}$ . The density evaluated at a specific point  $x$ , will be denoted, for instance for the gamma case, as  $\text{Ga}(x \mid \alpha, \beta)$ .

### 3 Four-way tail dependence

In what follows, we illustrate the four-way mixture using the Clayton copula but the construction is general and can be applied to other copula families.

Let  $C$  be a copula in the Clayton family, indexed by parameter  $\theta$  and defined as  $C(u_1, u_2) = (u_1^{-\theta} + u_2^{-\theta} - 1)^{-1/\theta}$  for  $\theta \geq -1$ . If  $\theta = 0$  Clayton copula reduces to the independence copula and for  $\theta > 0$  the lower-lower tail coefficient is  $\lambda_{LL} = 2^{-1/\theta}$ , and the Kendall's tau association parameter is  $\tau = \theta/(2 + \theta)$ . Furthermore, the Clayton family is in the class of Archimedean copulas with generator  $\varphi(t) = t^{-\theta} - 1$ .

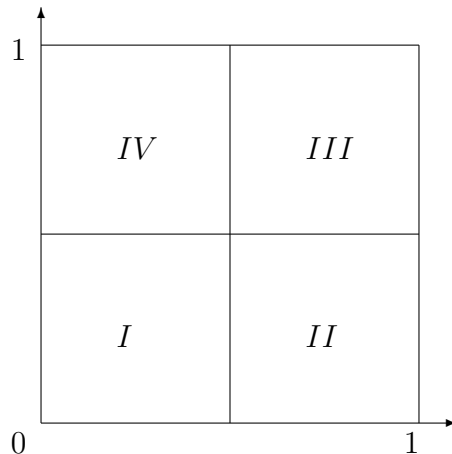


Figure 1: Unit square divided in four quadrants.

To understand the rotations, let us consider the unit square  $[0, 1]^2$  and divide it into four quadrants as in Figure 1. To define the 90-degree rotation, we consider the probability in quadrant II,  $P(U_1 > u_1, U_2 \leq u_2) = P(U_2 \leq u_2) - P(U_1 \leq u_1, U_2 \leq u_2)$ , which in terms of the copula becomes  $u_2 - C(u_1, u_2)$ . Finally by making the transformation  $U'_1 = 1 - U_1$ , we maintain the marginal uniformity in  $U'_1$  and can obtain a new CDF (copula) of the form

$$C_{II}(u_1, u_2) = P(U'_1 \leq u_1, U_2 \leq u_2) = u_2 - C(1 - u_1, u_2).$$

To define the 180-degree rotation, we consider the probability in the quadrant III,  $P(U_1 >$

$u_1, U_2 > u_2) = 1 - P(U_1 \leq u_1) - P(U_2 \leq u_2) + P(U_1 \leq u_1, U_2 \leq u_2)$ , which in terms of the copula becomes  $1 - u_1 - u_2 + C(u_1, u_2)$ . Again, making the transformation  $U'_1 = 1 - U_1$  and  $U'_2 = 1 - U_2$  we get a new CDF (copula)

$$C_{III}(u_1, u_2) = P(U'_1 \leq u_1, U'_2 \leq u_2) = u_1 + u_2 - 1 + C(1 - u_1, 1 - u_2).$$

Lastly, to define the 270-degree rotation we consider the probability in the quadrant IV,  $P(U_1 \leq u_1, U_2 > u_2) = P(U_1 \leq u_1) - P(U_1 \leq u_1, U_2 \leq u_2)$ , which in terms of the copula can be written as  $u_1 - C(u_1, u_2)$ . Making the transformation  $U'_2 = 1 - U_2$ , we obtain the new CDF (copula)

$$C_{IV}(u_1, u_2) = P(U_1 \leq u_1, U'_2 \leq u_2) = u_1 - C(u_1, 1 - u_2).$$

For completeness, we denote the original, un-rotated, copula as  $C_I(u_1, u_2)$ .

It is not difficult to prove that each of the previous four rotated copulas have the same tail dependence coefficients, but in different corners, i.e., lower-lower tail coefficient for copula  $I$ , upper-lower tail coefficient for copula  $II$ , upper-upper tail coefficient for copula  $III$  and lower-upper tail coefficient for copula  $IV$  are the same. Using (1), the tail coefficients become

$$\lambda_{LL}^I = \lambda_{UL}^{II} = \lambda_{UU}^{III} = \lambda_{LU}^{IV} = \lim_{\nu \rightarrow 0} \frac{(2\nu^{-\theta} - 1)^{-1/\theta}}{\nu} = \lim_{\nu \rightarrow 0} (2 - \nu^\theta)^{-1/\theta} = 2^{-1/\theta}, \quad (2)$$

for  $\theta > 0$ , and any other tail dependence coefficients are zero for the four rotated copulas.

## 4 Dynamic Clayton mixtures

Let  $(U_{1t}, U_{2t})$  be a bivariate vector with  $\text{Unif}(0, 1)$  marginal distributions for each  $U_{jt}$ , for  $j = 1, 2$  and  $t = 1, 2, \dots, T$ . The idea is to characterise the joint distribution between  $U_{1t}$  and  $U_{2t}$  through a flexible copula  $C_t$  which is able to capture any kind of tail dependence as it evolves in time. For that we define the following mixture copula

$$C_t(u_{1t}, u_{2t} \mid \boldsymbol{\pi}_t, \boldsymbol{\theta}_t) = \sum_{k=1}^4 \pi_{tk} C_k(u_{1t}, u_{2t}, \mid \theta_{tk}), \quad (3)$$

with parameters  $\boldsymbol{\pi}_t = (\pi_{t1}, \dots, \pi_{t4})$  and  $\boldsymbol{\theta}_t = (\theta_{t1}, \dots, \theta_{t4})$ , where  $C_k$  is a rotated Clayton copula as defined in Section 3, but expressed in arabic numbers instead of roman numbers for simplicity, with a different association parameter  $\theta_{tk} > 0$  for each rotated copula  $k = 1, \dots, 4$ . Specifically,

$$\begin{aligned}
C_1(u_1, u_2 | \theta_1) &= (u_1^{-\theta_1} + u_2^{-\theta_1} - 1)^{-1/\theta_1}, \\
C_2(u_1, u_2 | \theta_2) &= u_2 - \{(1 - u_1)^{-\theta_2} + u_2^{-\theta_2} - 1\}^{-1/\theta_2}, \\
C_3(u_1, u_2 | \theta_3) &= u_1 + u_2 - 1 + \{(1 - u_1)^{-\theta_3} + (1 - u_2)^{-\theta_3} - 1\}^{-1/\theta_3}, \\
C_4(u_1, u_2 | \theta_4) &= u_1 - \{u_1^{-\theta_4} + (1 - u_2)^{-\theta_4} - 1\}^{-1/\theta_4}.
\end{aligned} \tag{4}$$

Parameters  $\pi_{tk} > 0$  are mixture weights such that  $\pi_{t1} + \pi_{t2} + \pi_{t3} + \pi_{t4} = 1$  for  $t = 1, \dots, T$ .

It is not difficult to prove that association coefficients like the Kendall's tau and tail dependence coefficients for a mixture copula turn out to be the mixture of the individual coefficients. In particular, the Kendall's tau for the mixture copula (3) is

$$\begin{aligned}
\tau_t &= 4\mathbb{E}\{C_t(U_{1t}, U_{2t} | \boldsymbol{\pi}_t, \boldsymbol{\theta}_t)\} - 1 = 4 \sum_{k=1}^4 \pi_{tk} \mathbb{E}\{C_k(U_{1t}, U_{2t} | \boldsymbol{\theta}_t)\} - 1 \\
&= \sum_{k=1}^4 \pi_{tk} [4\mathbb{E}\{C_k(U_{1t}, U_{2t}, | \boldsymbol{\theta}_t)\} - 1] = \sum_{k=1}^4 \pi_{tk} \tau_{tk},
\end{aligned}$$

where  $\tau_{tk}$  is the individual Kendall's tau for each of the mixture copula components  $C_k$ . Since all mixture components  $C_k$  as in (4) are Clayton copulas, individual Kendall's tau coefficient are  $\tau_{tk} = \theta_{tk}/(2 + \theta_{tk})$  for  $k = 1, 3$  and  $\tau_k = -\theta_{tk}/(2 + \theta_{tk})$  for  $k = 2, 4$ . Therefore, the Kendall's tau coefficient for the mixture copula (3) becomes

$$\tau_t = \pi_{t1} \frac{\theta_{t1}}{2 + \theta_{t1}} - \pi_{t2} \frac{\theta_{t2}}{2 + \theta_{t2}} + \pi_{t3} \frac{\theta_{t3}}{2 + \theta_{t3}} - \pi_{t4} \frac{\theta_{t4}}{2 + \theta_{t4}}. \tag{5}$$

Now, tail dependence coefficients (1) for mixture copula (3) at time  $t$ , considering the

upper-upper tail, becomes

$$\begin{aligned}\lambda_{UU,t} &= \lim_{\nu \rightarrow 0} \frac{2\nu - 1 + C_t(1 - \nu, 1 - \nu)}{\nu} = \lim_{\nu \rightarrow 0} \frac{2\nu - 1 + \sum_{k=1}^4 \pi_{tk} C_k(1 - \nu, 1 - \nu)}{\nu} \\ &= \sum_{k=1}^4 \pi_{tk} \lim_{\nu \rightarrow 0} \left\{ \frac{2\nu - 1 + C_k(1 - \nu, 1 - \nu)}{\nu} \right\} = \sum_{k=1}^4 \pi_{tk} \lambda_{UU,t}^{(k)},\end{aligned}$$

where  $\lambda_{UU,t}^{(k)}$  is the individual upper-upper tail dependence coefficient for individual copula  $C_k$  at time  $t$ . Similar equations are obtained for the other three tail dependence coefficients. Therefore, considering that the only tail dependence coefficients for the mixture components of (3) are those in (2), the overall tail dependence coefficients in the case of the Clayton family are

$$\lambda_{LL,t} = \pi_{t1} 2^{-1/\theta_{t1}}, \quad \lambda_{UL,t} = \pi_{t2} 2^{-1/\theta_{t2}}, \quad \lambda_{UU,t} = \pi_{t3} 2^{-1/\theta_{t3}} \quad \text{and} \quad \lambda_{LU,t} = \pi_{t4} 2^{-1/\theta_{t4}}. \quad (6)$$

In summary, our mixture copula proposal (3) is flexible enough to capture a larger class of dependence associations and the four tail dependencies, according to the copula parameters  $\pi_{tk}$  and  $\theta_{tk}$  for  $k = 1, \dots, 4$  and  $t = 1, \dots, T$ .

## 5 Bayesian analysis

### 5.1 Prior distributions

To allow for temporal dependence in the parameter estimation, we propose a prior dynamic process for  $\boldsymbol{\pi} = \{\boldsymbol{\pi}_t\}$ , where  $\boldsymbol{\pi}_t = (\pi_{t1}, \pi_{t2}, \pi_{t3}, \pi_{t4})$  for  $t = 1, \dots, T$ . Since  $\sum_{k=1}^4 \pi_{tk} = 1$  for all  $t$ , the natural marginal prior for  $\boldsymbol{\pi}_t$  would be a Dirichlet distribution with parameter  $a_0 \mathbf{p}$ , where  $\mathbf{p} = (p_1, p_2, p_3, p_4)$  such that  $a_0 > 0$ ,  $p_k > 0$  and  $\sum_{k=1}^4 p_k = 1$ . To relate a set of Dirichlet random variables, we use ideas from [10] and define a dynamic prior with order of dependence  $q$  in the following way.

Let  $\boldsymbol{\eta}_t = (\eta_{t1}, \dots, \eta_{t4}) \in \mathbb{R}^4$  be a latent vector corresponding to each  $\boldsymbol{\pi}_t$  and let  $\boldsymbol{\omega} = (\omega_1, \dots, \omega_4)$  be a unique latent vector such that

$$\boldsymbol{\omega} \sim \text{Dir}(a_0 \mathbf{p}) \quad \text{and} \quad \boldsymbol{\eta}_t \mid \boldsymbol{\omega} \stackrel{\text{ind}}{\sim} \text{Mult}(a_t, \boldsymbol{\omega}), \quad (7)$$



with  $a_t \in \mathbb{N}$ ,  $\eta_{tk} \in \mathbb{N}$  and  $\sum_{k=1}^4 \eta_{tk} = a_t$ . Then, the prior dependence in  $\pi_t$  is modeled through  $q$  previous latent variables  $\eta_t, \eta_{t-1}, \dots, \eta_{t-q}$

$$\boldsymbol{\pi}_t \mid \boldsymbol{\eta} \stackrel{\text{ind}}{\sim} \text{Dir} \left( a_0 \mathbf{p} + \sum_{j=0}^q \boldsymbol{\eta}_{t-j} \right). \quad (8)$$

We denote this construction as  $\text{DDir}(q, a_0, \mathbf{a})$  with  $\mathbf{a} = (a_1, \dots, a_T)$ . Properties of this prior are given in the following proposition.

**Proposition 1** *Let  $\boldsymbol{\pi} = \{\boldsymbol{\pi}_t\} \sim \text{DDir}(q, a_0, \mathbf{a})$  a sequence of vectors whose probability law is defined by (7) and (8) for  $a_0 > 0$  and  $a_t \in \mathbb{N}$ . Then,*

(i) *The marginal distribution for each  $\boldsymbol{\pi}_t$  is  $\text{Dir}(a_0 \mathbf{p})$ ,*

(ii) *The correlation between  $\pi_{t,k}$  and  $\pi_{t+s,k}$  does not depend on  $k$  and is given by*

$$\text{Corr}(\pi_{t,k}, \pi_{t+s,k}) = \frac{a_0 \left( \sum_{j=0}^{q-s} a_{t-j} \right) + \left( \sum_{j=0}^q a_{t-j} \right) \left( \sum_{j=0}^q a_{t+s-j} \right)}{\left( a_0 + \sum_{j=0}^q a_{t-j} \right) \left( a_0 + \sum_{j=0}^q a_{t+s-j} \right)}$$

(iii) *If  $a_t = 0$  for all  $t = 1, \dots, T$  then the  $\boldsymbol{\pi}_t$ 's become independent.*

## Proof

For (i) we rely on conjugacy properties for the Dirichlet multinomial Bayesian updating [1]. This states that if  $\eta_t$ ,  $t = 1, 2, \dots$  are conditionally independent given  $\boldsymbol{\omega}$  from  $\text{Mult}(a_t, \boldsymbol{\omega})$ , and the prior distribution for  $\boldsymbol{\omega}$  is  $\text{Dir}(a_0 \mathbf{p})$ , then the posterior distribution for  $\boldsymbol{\omega}$  given the  $\eta_t$ 's is  $\text{Dir}(a_0 \mathbf{p} + \sum_t \boldsymbol{\eta}_t)$ . Replacing  $\boldsymbol{\omega}$  in the posterior by  $\boldsymbol{\pi}_t$  we obtain the marginal distribution for  $\boldsymbol{\pi}_t$  is the same as the prior for  $\boldsymbol{\omega}$  which is  $\text{Dir}(a_0 \mathbf{p})$ .

For (ii) we first note that for a specific  $k$ , the distributions for  $\omega_k$ ,  $\eta_{tk}$  and  $\pi_{tk}$  reduce to beta, binomial and beta, respectively. To obtain the correlation we rely on iterative formulae. The covariance is  $\text{Cov}(\pi_{t,k}, \pi_{t+s,k}) = \text{E}\{\text{Cov}(\pi_{t,k}, \pi_{t+s,k} \mid \boldsymbol{\eta})\} + \text{Cov}\{\text{E}(\pi_{t,k} \mid \boldsymbol{\eta}), \text{E}(\pi_{t+s,k} \mid \boldsymbol{\eta})\}$ , where the first term is zero due to conditional independence. Then

$$\text{Cov}(\pi_{t,k}, \pi_{t+s,k}) = \text{Cov} \left\{ \frac{a_0 p_k + \sum_{j=0}^q \eta_{t-j,k}}{a_0 + \sum_{j=0}^q a_{t-j}}, \frac{a_0 p_k + \sum_{j=0}^q \eta_{t+s-j,k}}{a_0 + \sum_{j=0}^q a_{t+s-j}} \right\},$$

which after cancelling the additive constants and using the linearity of the covariance we get

$$\text{Cov}(\pi_{t,k}, \pi_{t+s,k}) = \frac{1}{\left(a_0 + \sum_{j=0}^q a_{t-j}\right) \left(a_0 + \sum_{j=0}^q a_{t+s-j}\right)} \text{Cov} \left\{ \sum_{j=0}^q \eta_{t-j,k}, \sum_{j=0}^q \eta_{t+s-j,k} \right\}.$$

Working on the last covariance and using the iterative formula for a second time we get

$$\text{E} \left[ \text{Cov} \left\{ \sum_{j=0}^q \eta_{t-j,k}, \sum_{j=0}^q \eta_{t+s-j,k} \middle| \boldsymbol{\omega} \right\} \right] + \text{Cov} \left\{ \text{E} \left( \sum_{j=0}^q \eta_{t-j,k} \middle| \boldsymbol{\omega} \right), \text{E} \left( \sum_{j=0}^q \eta_{t+s-j,k} \middle| \boldsymbol{\omega} \right) \right\}.$$

Working on the sums and separating them in the common part as  $\sum_{j=0}^q \eta_{t-j,k} = \sum_{j=0}^{q-s} \eta_{t-j,k} + \sum_{j=q-s+1}^q \eta_{t-j,k}$  and  $\sum_{j=0}^q \eta_{t+s-j,k} = \sum_{j=0}^{s-1} \eta_{t+s-j,k} + \sum_{j=0}^{q-s} \eta_{t-j,k}$  and using covariance properties and conditional independence, the previous expression becomes

$$\text{E} \left\{ \text{Var} \left( \sum_{j=0}^{q-s} \eta_{t-j,k} \middle| \omega_k \right) \right\} + \text{Cov} \left\{ \sum_{j=0}^q a_{t-j} \omega_k, \sum_{j=0}^q a_{t+s-j} \omega_k \right\}.$$

The first expected value, after obtaining the conditional variance is  $\text{E}\{\sum_{j=0}^{q-s} a_{t-j} \omega_k (1 - \omega_k)\} = (\sum_{j=0}^{q-s} a_{t-j}) \text{E}(\omega_k - \omega_k^2) = \text{E}(\omega_k) - \text{E}^2(\omega_k) - \text{Var}(\omega_k) = a_0 \text{Var}(\omega_k)$ , the second term is  $(\sum_{j=0}^q a_{t-j})(\sum_{j=0}^q a_{t+s-j}) \text{Var}(\omega_k)$ . Finally,

$$\text{Cov}(\omega_{t,k}, \omega_{t+s,k}) = \frac{a_0 \left( \sum_{j=0}^{q-s} a_{t-j} \right) + \left( \sum_{j=0}^q a_{t-j} \right) \left( \sum_{j=0}^q a_{t+s-j} \right)}{\left( a_0 + \sum_{j=0}^q a_{t-j} \right) \left( a_0 + \sum_{j=0}^q a_{t+s-j} \right)} \text{Var}(\omega_k).$$

Since  $\omega_k$ ,  $\pi_{t,k}$  and  $\pi_{t+s,k}$  all have the same beta marginal distribution, we obtain the result.

For (iii) we note that  $a_t = 0$  for all  $t$  implies that  $\boldsymbol{\eta}_t = 0$  with probability one so the dependence disappears and  $\boldsymbol{\pi}_t$  become independent with marginal distribution  $\text{Dir}(a_0 \mathbf{p})$ .  $\diamond$

The strength of dependence in the prior for  $\boldsymbol{\pi}$  depends on the model parameters  $q$ ,  $a_0$  and  $\mathbf{a}$ . Larger values of any of these three parameters induce stronger dependence. Prior distributions are completed by assigning hierarchical gamma distributions for each  $\theta_{tk}$ , so that information is shared across times  $t$  for each  $k$ . That is,

$$\theta_{tk} \mid \beta_k \stackrel{\text{ind}}{\sim} \text{Ga}(d_k, \beta_k), \quad t = 1, \dots, T \quad \text{and} \quad \beta_k \sim \text{Ga}(e_k, g_k) \quad (9)$$

for  $k = 1, \dots, 4$ .

## 5.2 Posterior distributions

Let  $\mathbf{U}_{ti} = (U_{1ti}, U_{2ti})$  for  $i = 1, \dots, n_t$  a sample of size  $n_t$  from model (3) for each  $t = 1, \dots, T$ . Let  $\mathbf{Z}_{ti}$  be a latent vector that identifies from what mixture component observation  $i$  is coming from, that is,  $\mathbf{Z}'_{ti} = (Z_{t1i}, Z_{t2i}, Z_{t3i}, Z_{t4i}) \sim \text{Mult}(1, \boldsymbol{\pi}_t)$ . Assuming for the moment that together with  $\mathbf{U}_{ti}$  we observe  $\mathbf{Z}_{ti}$ , then the extended likelihood has the form

$$f(\mathbf{u}, \mathbf{z} \mid \boldsymbol{\pi}, \boldsymbol{\theta}) = \prod_{t=1}^T \prod_{i=1}^{n_t} \prod_{k=1}^4 \{\pi_{tk} f_k(u_{1ti}, u_{2ti} \mid \theta_{tk})\}^{z_{tki}},$$

where

$$\begin{aligned} f_1(u_1, u_2 \mid \theta_1) &= (\theta_1 + 1)(u_1 u_2)^{-(\theta_1+1)} (u_1^{-\theta_1} + u_2^{-\theta_1} - 1)^{-(1/\theta_1+2)}, \\ f_2(u_1, u_2 \mid \theta_2) &= (\theta_2 + 1)\{(1 - u_1)u_2\}^{-(\theta_2+1)} \{(1 - u_1)^{-\theta_2} + u_2^{-\theta_2} - 1\}^{-(1/\theta_2+2)}, \\ f_3(u_1, u_2 \mid \theta_3) &= (\theta_3 + 1)\{(1 - u_1)(1 - u_2)\}^{-(\theta_3+1)} \{(1 - u_1)^{-\theta_3} + (1 - u_2)^{-\theta_3} - 1\}^{-(1/\theta_3+2)}, \\ f_4(u_1, u_2 \mid \theta_4) &= (\theta_4 + 1)\{u_1(1 - u_2)\}^{-(\theta_4+1)} \{u_1^{-\theta_4} + (1 - u_2)^{-\theta_4} - 1\}^{-(1/\theta_4+2)}. \end{aligned} \quad (10)$$

The prior distribution for  $(\boldsymbol{\pi}, \boldsymbol{\theta})$  is defined by equations (7), (8) and (9). Again, extending the prior to include the latent variables  $\boldsymbol{\eta}$  and  $\boldsymbol{\omega}$  we get

$$f(\boldsymbol{\pi}, \boldsymbol{\eta}, \boldsymbol{\omega}) = \text{Dir}(\boldsymbol{\omega} \mid a_0 \mathbf{p}) \prod_{t=1}^T \text{Dir} \left( \boldsymbol{\pi}_t \mid a_0 \mathbf{p} + \sum_{j=0}^q \boldsymbol{\eta}_{t-j} \right) \text{Mult}(\boldsymbol{\eta}_t \mid a_t, \boldsymbol{\omega})$$

and

$$f(\boldsymbol{\theta}) = \prod_{k=1}^4 \text{Ga}(\beta_k \mid e_k, g_k) \prod_{t=1}^T \text{Ga}(\theta_{tk} \mid d_k, \beta_k)$$

independent of each other.

Posterior distributions are characterised through their full conditional distributions. These include actual parameters as well as latent variables and are given as follows.

- (a) The posterior conditional for  $\mathbf{Z}_{ti}$  is

$$\mathbf{Z}_{ti} \mid \text{rest} \sim \text{Mult}(1, \boldsymbol{\pi}_t^*),$$

where  $\boldsymbol{\pi}^* = \{\pi_{tk}^*\}$  and

$$\pi_{tk}^* = \frac{\pi_{tk} f_k(u_{1ti}, u_{2ti} | \theta_{tk})}{\sum_{j=1}^4 \pi_{tj} f_j(u_{1ti}, u_{2ti} | \theta_{tj})},$$

with  $f_k$  is given in (10) for  $k = 1, \dots, 4$ .

(b) The posterior conditional for  $\boldsymbol{\pi}_t$  is

$$\boldsymbol{\pi}_t | \text{rest} \sim \text{Dir} \left( a_0 \mathbf{p} + \sum_{j=0}^q \boldsymbol{\eta}_{t-j} + \sum_{i=1}^{n_t} \mathbf{z}_{ti} \right).$$

(c) The posterior conditional for  $\boldsymbol{\eta}_t$  is

$$f(\boldsymbol{\eta}_t | \text{rest}) \propto \left\{ \prod_{k=1}^4 \frac{(\omega_k \prod_{l=0}^q \pi_{t+l,k})^{\eta_{tk}}}{\Gamma(\eta_{tk} + 1) \prod_{l=0}^q \Gamma(a_0 p_k + \sum_{j=0}^q \eta_{t+l-j,k})} \right\} I \left( \sum_{k=1}^4 \eta_{tk} = a_t \right).$$

(d) The posterior conditional for  $\boldsymbol{\omega}$  is

$$f(\boldsymbol{\omega} | \text{rest}) = \text{Dir} \left( \boldsymbol{\omega} \left| c_0 \mathbf{p} + \sum_{t=1}^T \boldsymbol{\eta}_t \right. \right).$$

(e) The posterior conditional for  $\theta_{tk}$  is

$$f(\theta_{tk} | \text{rest}) \propto \theta_{tk}^{d_k - 1} e^{-\beta_k \theta_{tk}} \prod_{i=1}^{n_t} \{f_k(u_{1ti}, u_{2ti} | \theta_{tk})\}^{z_{tki}},$$

where  $f_k$  is given in (10).

(f) The posterior conditional for  $\beta_k$  is

$$\beta_k | \text{rest} \sim \text{Ga} \left( e_k + T d_k, g_k + \sum_{t=1}^T \theta_{tk} \right).$$

Posterior inference will rely on the implementation of a Gibbs sampler [13] based on the previous posterior conditional distributions. Sampling from (a), (b), (d) and (f) is straightforward since they are of standard form. To sample from (c), since  $\boldsymbol{\eta}_t$  is a vector of

dimension 4 with a sum restriction, it is easier if we sample from each of the components  $\eta_{tk}$  for  $k = 1, 2, 3$  from  $f(\eta_{tk} \mid \text{rest}) \propto$

$$\frac{\{\omega_k \prod_{l=0}^q \pi_{t+l,k} / (\omega_4 \prod_{l=0}^q \pi_{t+l,4})\}^{\eta_{tk}} I\left(\eta_{tk} \in \{0, 1, \dots, a_t - \sum_{j \neq k}^3 \eta_{tj}\}\right)}{\Gamma(\eta_{tk} + 1) \prod_{l=0}^q \Gamma\left(a_0 p_k + \sum_{j=0}^q \eta_{t+l-j,k}\right) \Gamma(\eta_{t4} + 1) \prod_{l=0}^q \Gamma\left(a_0 p_4 + \sum_{j=0}^q \eta_{t+l-j,4}\right)},$$

with  $\eta_{t4} = a_t - \sum_{j=1}^3 \eta_{tj}$ . Sampling from (e) will require a Metropolis-Hastings step [15].

We suggest to use an adaptive random walk proposal defined as follows. At iteration  $(s + 1)$  sample  $\theta_{tk}^* \sim \text{Ga}(\kappa, \kappa/\theta_{tk}^{(s)})$  and accept it with probability

$$\alpha(\theta_{tk}^*, \theta_{tk}^{(s)}) = \frac{f(\theta_{tk}^* \mid \text{rest}) \text{Ga}(\theta_{tk}^{(s)} \mid \kappa, \kappa/\theta_{tk}^*)}{f(\theta_{tk}^{(s)} \mid \text{rest}) \text{Ga}(\theta_{tk}^* \mid \kappa, \kappa/\theta_{tk}^{(s)})},$$

where  $\alpha$  is truncated to the interval  $[0, 1]$  and  $\kappa$  is a tuning parameter that controls the acceptance rate. We adapt  $\kappa$  following the method of [9]. The adaptation method uses batches of 50 iterations and for every batch  $h$  we compute the acceptance rate  $AR^{(h)}$  and increase  $\kappa^{(h+1)} = \kappa^{(h)} 1.01^{\sqrt{h}}$  if  $AR^{(h)} < 0.3$  and decrease  $\kappa^{(h+1)} = \kappa^{(h)} 1.01^{-\sqrt{h}}$  if  $AR^{(h)} > 0.4$ , with  $\kappa^{(1)} = 1$  as starting value.

## 6 Numerical analyses

### 6.1 Simulation study

We conduct a comprehensive simulation study to evaluate the performance of the proposed model.

The true generative model is set as following:  $\theta_t = (\theta_{t1}, \theta_{t2}, \theta_{t3}, \theta_{t4}) = (5, 3, 4, 3)$  for  $t = 1, \dots, T$ , with  $T = 20$ . The weights of rotated Clayton copulas are chosen to be linearly dependent in time. More specifically, we first set  $\boldsymbol{\pi}_1 = (\pi_{11}, \pi_{12}, \pi_{13}, \pi_{14}) = (0.4, 0.25, 0.1, 0.25)$  as the initial values at  $t = 1$  and subsequently the weights are constructed using  $\pi_{t1} = 0.95\pi_{t-1,1}$ ,  $\pi_{t1} = 1.05\pi_{t-1,2}$ ,  $\pi_{t3} = 0.1$ ,  $\pi_{t4} = 1 - \sum_{i=1}^3 \pi_{ti}$  for  $t = 2, \dots, 20$ . We sampled  $n_t = 300$  realizations from this model for each time  $t = 1, \dots, T$  as the simulated data.

For the prior distributions, we set hyper-parameters  $a_0 = 1$ , and  $e_k = g_k = 1$ . To evaluate the performance of the model for capturing the temporal dependence, we ran the model with different hyper-parameters for the dynamic process:  $a_t = 0, 1, 3, 5, 10, 20, 30, 40$ , and  $q = 0, 1, \dots, 7$ . We ran the MCMC for 7,000 iterations. To determine the burn-in, we monitor the adaptive  $\kappa$  parameter and the acceptance rate for each batch. These are included in Figure 2 where we observe that the  $\kappa$  becomes stable after 60 batch iterations, and the acceptance rate stabilizes between 0.3 and 0.4 after 60 batches. Therefore we set the burn-in to be equal to 3,000 iterations. This also confirms that the adaptation method proposed performs well.

To assess model performance, we computed two goodness (gof) of fit measures, the deviance information criterion (DIC) [14] and the logarithm of the pseudo marginal likelihood (LPML) [4]. Tables 1 and 2 show these values. In general, both gof measures concur in determining the best model for each value of  $q$ . Briefly put, for smaller values of  $a_t$ , better fitting is achieved for larger orders of dependence  $q$  in the  $\pi_{tk}$ , whereas for larger values of  $a_t$ , smaller orders of dependence  $q$  produce better fit. Overall, the best model is obtained with  $a_t = 30$  and  $q = 2$ .

Two more comparisons are included in Tables 1 and 2. The independence case across times for  $\pi_{tk}$ , obtained when  $a_t = 0$ , regardless of the value of  $q$ . Goodness of fit statistics show that the independence fitting is not the worst, but is definitely overcome by many other dependence models. Additionally, we also compare with the fitting obtained when assuming independence in the  $\theta_{tk}$ . This is achieved by considering a very low variance in  $\beta_k$ , which is obtained by setting  $e_k = d_k = 1000$ . Fitting measures when assuming exchangeability in the  $\theta_{tk}$  is a lot better than the one obtained with the low variance.

To assess in more detail our model's performance, we compare posterior estimates of  $\boldsymbol{\pi}$  and  $\boldsymbol{\theta}$  with the true values. We use the best fitting model and use posterior means as point estimates, together with quantiles 2.5% and 97.5% to produce 95% credible intervals.

Figure 3 shows posterior estimates of  $\pi_{tk}$  as time series for  $t = 1, \dots, 20$  in four panels for  $k = 1, \dots, 4$ . Posterior estimates follow very closely the path of the true values. Similarly, Figure 4 shows posterior estimates of  $\theta_{tk}$  as time series in four panels. All the true values lie within the 95% credible intervals. We note that credible intervals are narrower for  $\theta_{t1}$  (top-left panel) and  $\theta_{t4}$  (bottom-right panel) as compared to those for  $\theta_{t2}$  (top-right panel) and  $\theta_{t3}$  (bottom-left panel). Wider credible intervals are due to smaller weights (less data points) associated to the corresponding mixture components. Specifically, the higher variability for  $\theta_{t3}$  for larger  $t$  is a consequence of the smaller weights for the third component  $\pi_{t3}$ .

## 6.2 Real data analysis

We also assessed how well our model can capture the relationship between variables in a real life application where data is generated from some unknown distribution, rather than directly from a mixture copula.

We used the Environment and Climate Change Canada Data Catalogue (ECCC) from the Government of Canada. The ECCC managed the National Air Pollution Surveillance (NAPS) Program, which began in 1969 and is now comprised of nearly 260 stations in 150 rural and urban communities reporting to the Canada-Wide Air Quality Database (for more details about the dataset, please visit <https://data-donnees.az.ec.gc.ca/data/air/monitor>).

Specifically, we selected the ozone ( $O_3$ ) and particulate matter with diameters 2.5 and smaller ( $PM_{2.5}$ ) as the bivariate data. We used the hourly data from the years 2017 to 2019. Due to a large number of missing values, we took averages across hours and across days to produce monthly data for each station,  $t = 1, \dots, T$  with  $T = 36$  for a total time span of three years. The number of stations varies across months, given that some of them have missing values for the whole month. In average, sample sizes range around  $n_t \approx 200$  for each  $t$ .

Since our objective is not the marginal distributions, but the association between these

two variables, we applied the modified rank transformation (inverse empirical cdf) to produce data in the interval  $[0, 1]$ . To explore the data, we computed empirical Kendall’s tau and Spearman’s rho association coefficients per month. These are shown in Figure 2. In both cases the dependence is cyclical around zero, reaching its maximum in June/July and its minimum in October/November. This suggests that our model seems to be a good candidate to capture these cycles.

Similar to the simulation study, we set the parameters  $a_0 = 1$  and  $b_k = c_k = 1$  to define the prior distributions. In this real data analysis, we also varied the dependence parameters  $a_t = 0, 1, \dots, 5$  and  $q = 0, 1, \dots, 4$  to assess the performance of the model under different strengths of temporal dependence. We ran the MCMC for 10,000 iterations and set the burn-in equal to 2,500. We also used DIC and LPML statistics to assess goodness of fit.

Table 3 and 4 show the DIC and LPML values for the different prior specifications. We observed that modelling the temporal dependence appropriately achieved higher performance. For example, the model with parameters  $a_t = 1$  and  $q = 3$  had better goodness of fit than the model that assumes independence in the weights ( $a_t = 0$ ).

In Figures 6 and 7 we show posterior estimates of the weights  $pi_{tk}$  and copula coefficients  $\theta_{tk}$ , respectively. The cyclical monthly dependence is captured by the weights. Since the first and third components of the mixture induce positive dependence, and second and fourth induce negative dependence, there is an opposite behaviour between the pairs  $(\pi_{t1}, \pi_{t3})$  and  $(\pi_{t2}, \pi_{t4})$ . The former reaches its peak in the summer and the latter in the winter. Among the four components, component 3 is the one with smaller weights, apart from the summer of the year 2019 where  $\pi_{t3}$  reaches its maximum of around 0.5. Therefore, it seems that the positive dependence is mostly driven by the first component and the negative dependence by both second and fourth components.

The strength of the dependence is determined by parameters  $\theta_{tk}$ . Their posterior estimates are all around the value of one, apart from  $\theta_{t1}$ , which shows lower values. Uncertainty



in the estimation of  $\theta_{t3}$  is particularly high, due to the smaller weight  $\pi_{t3}$  and thus smaller sample size for estimating  $\theta_{t3}$ . According to  $\theta_{t1}$ , positive dependence is particularly high in the summer of the years 2017 and 2019 with a lower-lower tail dependence. On the other hand, looking at  $\theta_{2t}$  and  $\theta_{4t}$ , negative dependence is high in the winter of the three years with both upper-lower and lower-upper tail dependencies.

We perform a validation study by partitioning the dataset into two sets, fitting and testing. For each month  $t = 1, \dots, T$  we took  $n_{t1} = 140$  for fitting and  $n_{t2} = n_t - 140$  for testing. We estimate the model parameters with the fitting set and use the testing set to predict  $O_3$  conditional on the observed value of  $PM_{2.5}$ . For this we use the conditional copula  $C_t(u_{1t} | u_{2t}, \boldsymbol{\pi}_t, \boldsymbol{\theta}_t) = \sum_{k=1}^4 \pi_{tk} C_k(u_{2t} | u_{1t}, \theta_{tk})$  with  $C_k(u_{2t} | u_{1t}, \theta_{tk}) = (\partial/\partial u_{1t}) C_k(u_{1t}, u_{2t} | \theta_{tk})$  for  $k = 1, \dots, 4$ , and obtain the posterior predictive mean  $\hat{u}_{2t} = E(U_{2t} | u_{1t}, \boldsymbol{\pi}_t, \boldsymbol{\theta}_t)$ .

We assess model performance by computing the mean square error between the observed  $u_{t2}$  and predicted  $\hat{u}_{t2}$  for  $O_3$  in the test set, i.e.  $MSE = \left( \sum_{t=1}^T n_{t2} MSE_t \right) / \left( \sum_{t=1}^T n_{t2} \right)$ , where  $MSE_t = (1/n_{t2}) \sum_{i=1}^{n_{t2}} (u_{t2} - \hat{u}_{t2})^2$ . We compare with the MSE obtained by assuming a simple Clayton copula. Additionally we also compute the LPML and DIC goodness of fit measures for the fitting sets of our mixture model and simple Clayton copula.

Results from the validation study are included in Table 5. All three gof statistics of our mixture model are a lot better than those obtained for a single Clayton copula, confirming that our model is superior.

Finally, we show joint density estimates in Figure 8 as heat plots, together with scatter plots of the data for each month  $t$ . We particularly concentrate on the months where the dependence changes from negative to positive. This transition is consistent along the three years of study for the months of June and July. It is interesting to see that August is a transition month, where in 2017 and 2019 the dependence is 4-way, i.e., the four mixture components of our model are present, in fact the estimated weights and coefficients are:  $\boldsymbol{\pi}_{2017-8} = (0.54, 0.40, 0.02, 0.04)$ ,  $\boldsymbol{\theta}_{2017-8} = (0.45, 0.88, 0.87, 0.86)$ ;  $\boldsymbol{\pi}_{2018-8} =$

$(0.43, 0.48, 0.02, 0.08)$ ,  $\boldsymbol{\theta}_{2018-8} = (0.13, 0.52, 0.84, 0.84)$ ;  $\boldsymbol{\pi}_{2019-8} = (0.62, 0.28, 0.04, 0.05)$ ,  $\boldsymbol{\theta}_{2019-8} = (0.15, 0.51, 0.84, 0.84)$ . What makes the heat plots to show the 4-way dependence is a combination of the weight  $\pi_{tk}$  and the intensity  $\theta_{tk}$ .

## 7 Concluding remarks and future work

We extend a copula's versatility via mixtures of copulas. The idea is illustrated using the Clayton copulas, but can be applied to any other family. The motivation is given by problems where different extremal regions of the bivariate distribution exhibit patterns that cannot be captured by a single copula. For situations in which the dependence varies in time we propose a dynamic mixture of copulas model in which the mixture weights and the parameters of the copulas involved in the mixture are modelled to account for a dynamic regime. This added flexibility is illustrated by all our numerical experiments, be they synthetic or real.

Future work will explore extensions of these ideas to higher dimensions. For instance, one can easily see that if we were to capture dependence in all the extreme regions of a 10-dimensional copula, we would need 100 mixture components, each component being a 10-dimensional copula. Although feasible, such an approach is likely impractical as not all extremes are likely to be significant. In order to impose sparsity, we plan to exploit a Dirichlet process mixture prior to reduce the number of components needed to model the data and yet maintain the added flexibility demonstrated in this work. An added question of interest is the identification of lower dimensional manifolds where a mixture of lower-dimensional copulas can be used to capture the dependence in the data.

## Acknowledgements

This work was supported by *Asociación Mexicana de Cultura, A.C.* while the second author was visiting the Department of Statistical Sciences at the University of Toronto and by an NSERC of Canada discovery grant of the third author. We are also grateful to Jun Young

Park and Patrick Brown for their guidance on potential applications.

## References

- [1] Bernardo, J.M. and Smith, A.M.F. (2000). *Bayesian theory*. Wiley, London.
- [2] Czado, Claudia and Nagler, Thomas (2022). Vine copula based modeling. *Annual Review of Statistics and Its Application* **9**, 453–477.
- [3] Frahm, G., Junker, M. and Schmidt, R. (2005). Estimating the tail-dependence coefficient: Properties and pitfalls. *Insurance: Mathematics and Economics* **37**, 80–100.
- [4] Geisser, S. and Eddy, W.F. (1979). A predictive approach to model selection. *Journal of the American Statistical Association* **74**, 153–160.
- [5] Joe, H. (1997). *Multivariate models and dependence concepts*. Chapman and Hall, London.
- [6] Klein, N., Kneib, T., Marra, G. and Radice, R. (2020). Bayesian mixed binary-continuous copula regression with an application to childhood under nutrition. In *Flexible Bayesian regression modeling*. Y.Fan, D.Nott, M.S.Smith, J.L. Dortet-Bernadet (eds.) 121–152.
- [7] Longla, M. (2015). On mixtures of copulas and mixing coefficients. *Journal of Multivariate analysis* **139**, 259–265.
- [8] Nelsen, R.B. (2006). *An introduction to copulas*. Springer, New York.
- [9] Nieto-Barajas, L.E. (2024). Multivariate and regression models for directional data based on projected Pólya trees. *Statistics and Computing*. To appear.

- [10] Nieto-Barajas, L.E. and Gutiérrez-Peña, E. (2022). General dependence structures for some models based on exponential families with quadratic variance functions. *TEST* **31**, 699–716.
- [11] Silva, R. and Gramacy, R. (2009). MCMC methods for Bayesian mixtures of copulas. *Artificial Intelligence and Statistics*, PMLR, 512–519.
- [12] Sklar, A. (1959). Fonctions de répartition à n dimensions et leurs marges. *Publications de l'Institut de Statistique de l'Université de Paris* **8**, 229–231.
- [13] Smith, A. and Roberts, G. (1993). Bayesian computations via the Gibbs sampler and related Markov chain Monte Carlo methods. *Journal of the Royal Statistical Society, Series B* **55**, 3–23.
- [14] Spiegelhalter, D.J., Best, N.G., Carlin, B.P. and van der Linde, A. (2002). Bayesian measures of model complexity and fit (with discussion). *Journal of the Royal Statistical Society, Series B* **64**, 583–639.
- [15] Tierney, L. (1994). Markov chains for exploring posterior distributions. *Annals of Statistics* **22**, 1701–1722.
- [16] Tjøstheim, D., Otneim, H. and Støve, B. (2022). Local Gaussian correlation and the copula. In *Statistical Modeling Using Local Gaussian Approximation*. D.Tjøstheim, H.Otneim, B.Støve (eds.) Academic Press, 135–159.

$b_k, c_k$	$a_t$	$q = 0$	$q = 1$	$q = 2$	$q = 3$	$q = 4$	$q = 5$	$q = 6$	$q = 7$
1	0	-3384							
1	1	-3378	-3378	-3375	-3383	-3386	<b>-3392</b>	-3391	-3390
1	3	-3375	-3387	-3391	-3389	-3399	-3398	-3400	<b>-3402</b>
1	5	-3382	-3388	-3393	-3399	-3402	-3404	<b>-3405</b>	-3406
1	10	-3393	-3399	-3403	-3406	-3406	-3409	<b>-3410</b>	-3409
1	20	-3400	-3404	-3409	<b>-3411</b>	-3406	-3406	-3410	-3407
1	30	-3402	-3407	<b>-3413</b>	-3409	-3409	-3408	-3403	-3403
1	40	-3407	<b>-3408</b>	-3407	-3411	-3407	-3403	-3405	-3399
1000	30	-3363	-3372	-3380	-3380	-3379	-3378	-3374	-3370

Table 1: Simulated data. DIC values of different models. Smallest DIC for each  $a_t$  are shown in blue.

$b_k, c_k$	$a_t$	$q = 0$	$q = 1$	$q = 2$	$q = 3$	$q = 4$	$q = 5$	$q = 6$	$q = 7$
1	0	1687							
1	1	1685	1685	1684	1687	1690	1692	1691	<b>1693</b>
1	3	1684	1689	1694	1693	1697	1697	1699	<b>1700</b>
1	5	1686	1693	1697	1699	1700	1701	<b>1703</b>	1703
1	10	1695	1699	1701	1703	1703	1704	<b>1705</b>	1704
1	20	1696	1702	1704	<b>1706</b>	1702	1702	1703	1701
1	30	1700	1703	<b>1706</b>	1704	1703	1702	1700	1698
1	40	1701	1703	1703	<b>1704</b>	1702	1699	1698	1694
1000	30	1682	1687	1691	1691	1690	1689	1686	1686

Table 2: Simulated data. LPML values of different models. Largest LPML for each  $a_t$  are shown in blue.

$a_t$	$q = 0$	$q = 1$	$q = 2$	$q = 3$	$q = 4$
0	-791				
1	-791	-797	-802	<b>-804</b>	-802
2	-794	<b>-804</b>	-798	-794	-785
3	<b>-800</b>	-799	-792	-784	-776
4	-800	-798	-787	-771	-758
5	-798	-791	-779	-762	-747

Table 3: Real data. DIC values of different models.

$a_t$	$q = 0$	$q = 1$	$q = 2$	$q = 3$	$q = 4$
0	383				
1	384	388	393	393	392
2	386	392	391	388	383
3	387	390	386	383	379
4	386	388	384	378	375
5	386	385	382	375	368

Table 4: Real data. LPML values of different models.

Statistic	Dynamic Clayton mixtures	Simple Clayton
MSE	0.075	0.082
DIC	-734.4	-73.7
LPML	359.7	36.5

Table 5: Real data. Goodness of fit measures in validation study.

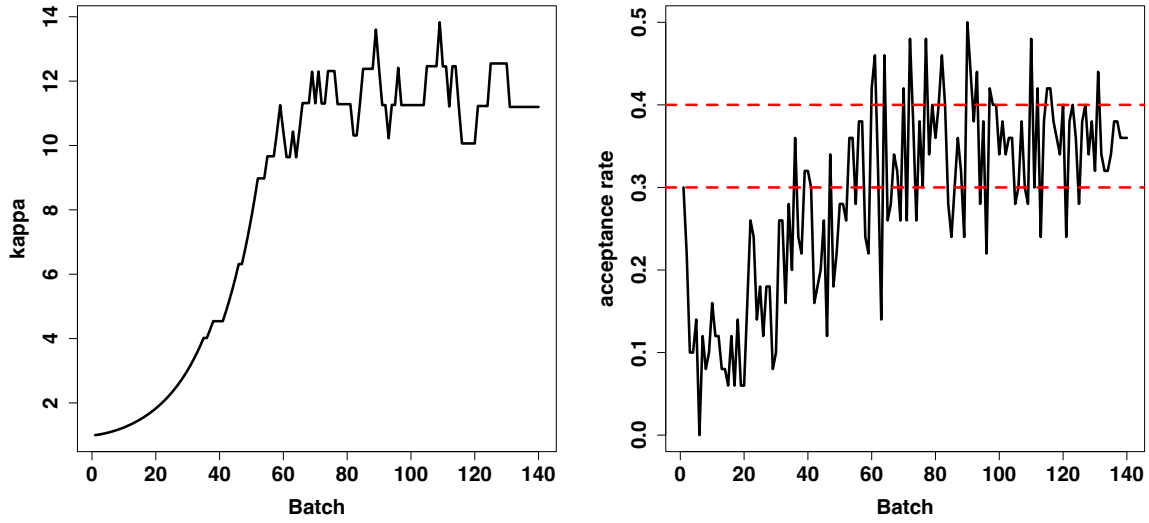


Figure 2: The recorded  $\kappa^{(h)}$  and acceptance rate for each batch  $h$ . The batch size is 50.

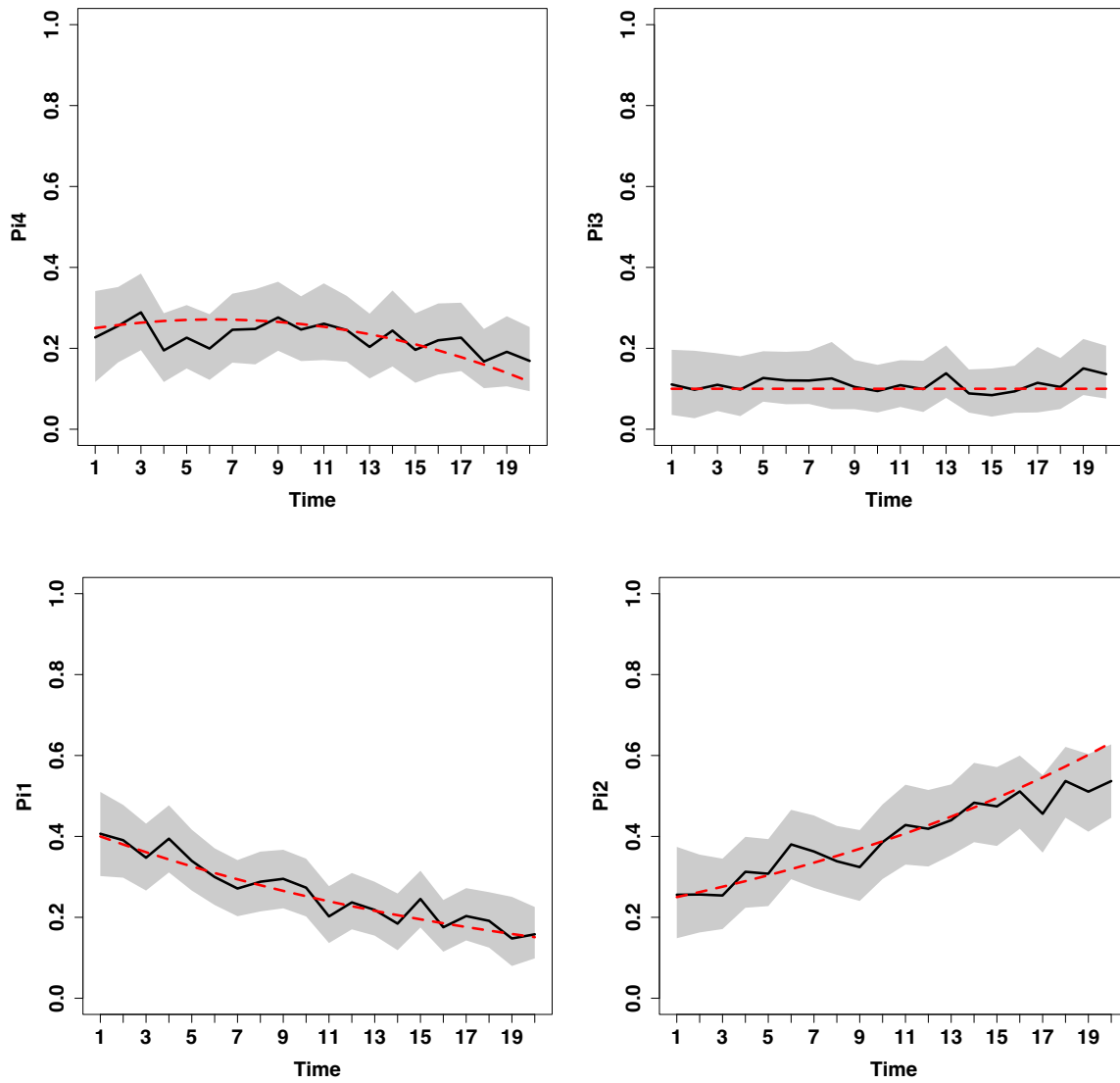


Figure 3: Simulated data. Posterior estimates of  $\pi$ : posterior mean (solid line) with 95% credible intervals (shadows), together with the true value (dotted red line).

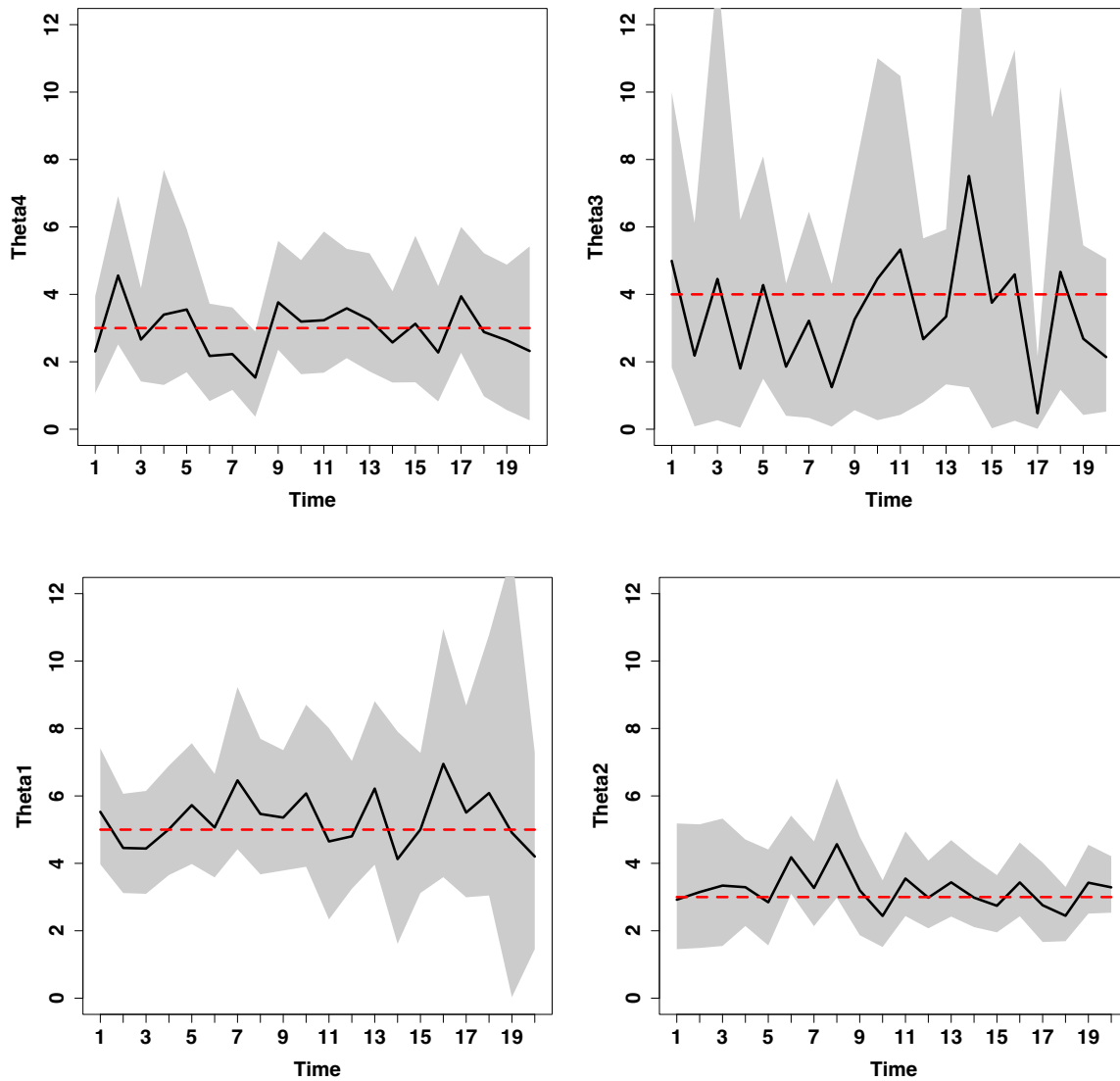


Figure 4: Simulated data. Posterior estimates of  $\theta$ : posterior mean (solid line) with 95% credible intervals (shadows), together with the true value (dotted red line).



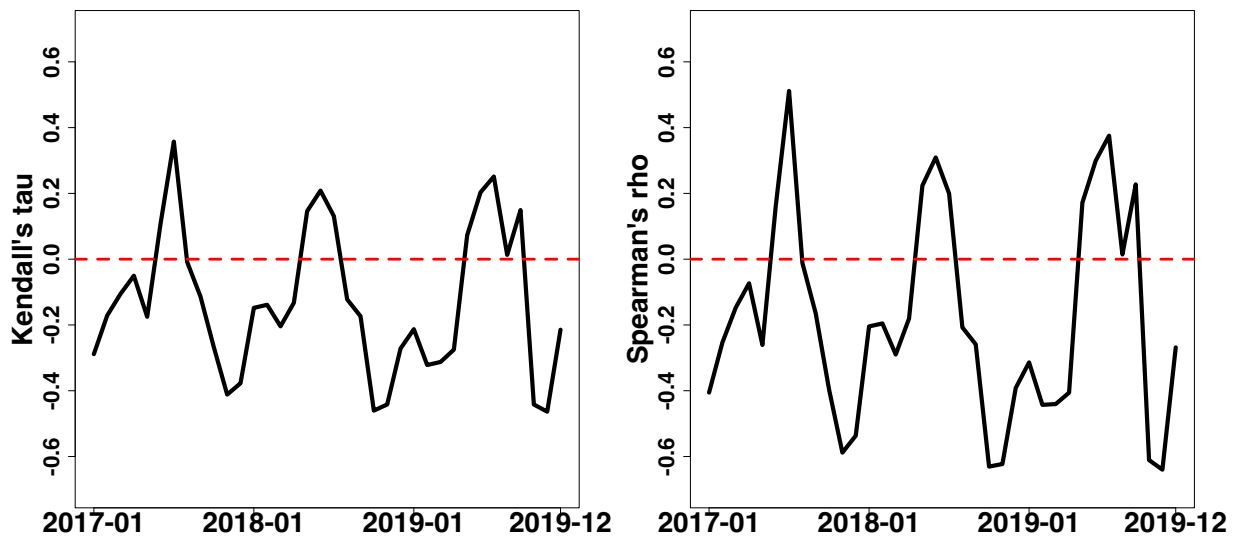


Figure 5: Real dataset. Empirical Kendall's tau (left) and Spearman's rho (right).

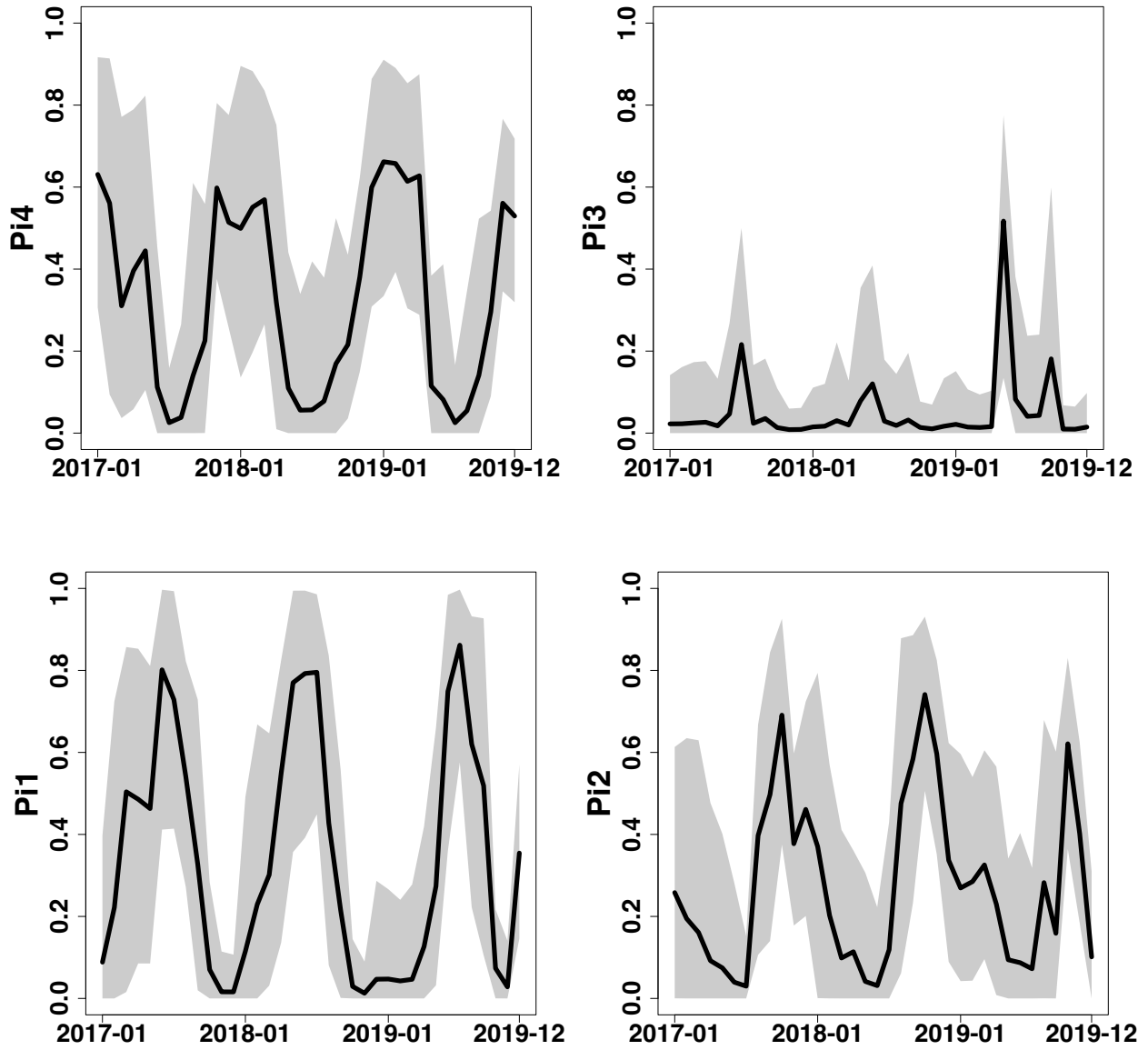


Figure 6: Real dataset. Posterior estimates of  $\pi$ : posterior mean (solid line) with 95% credible intervals (shadows).

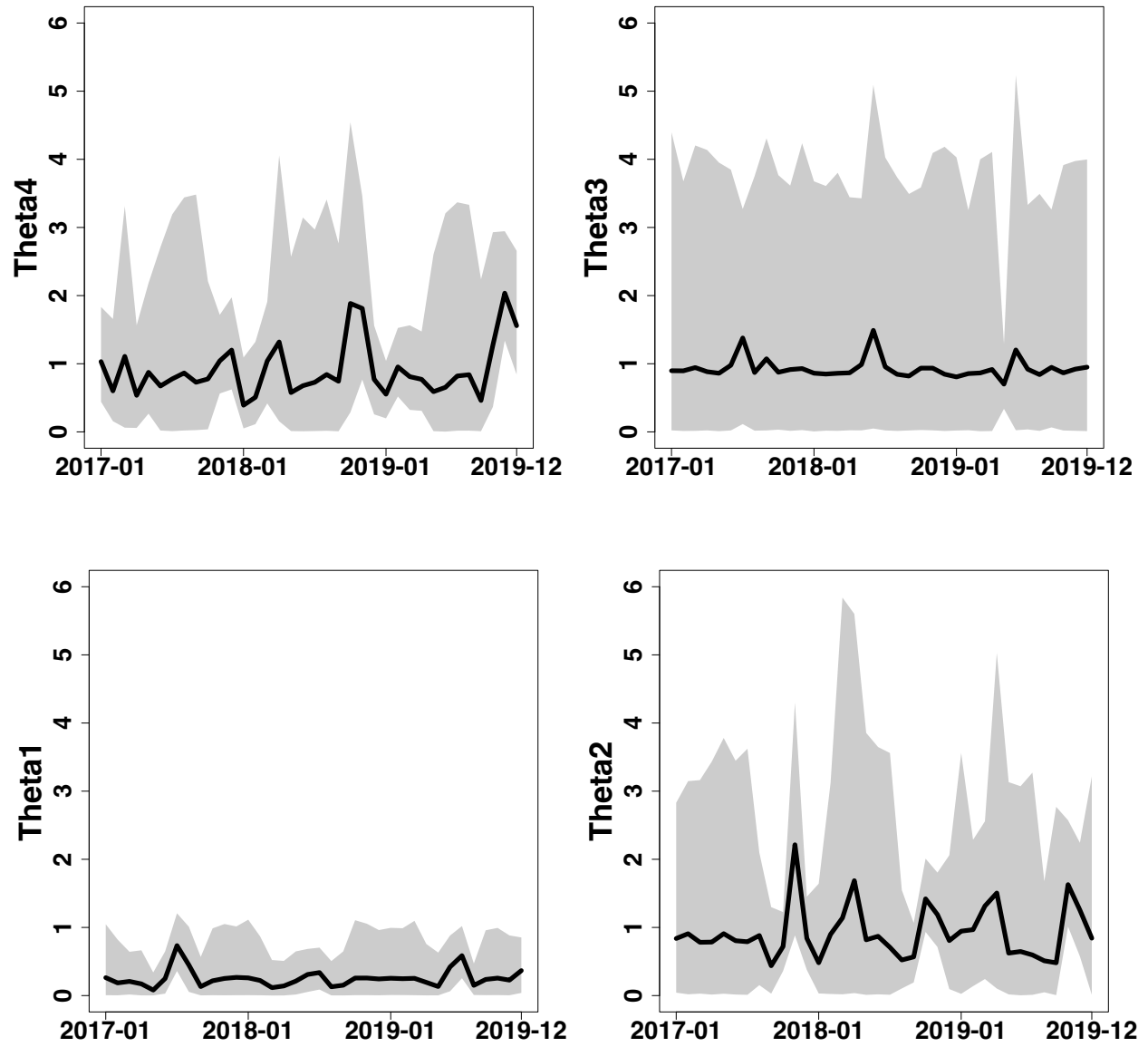


Figure 7: realdataset. Posterior estimates of  $\theta$ : posterior mean (solid line) with 95% credible intervals (shadows).

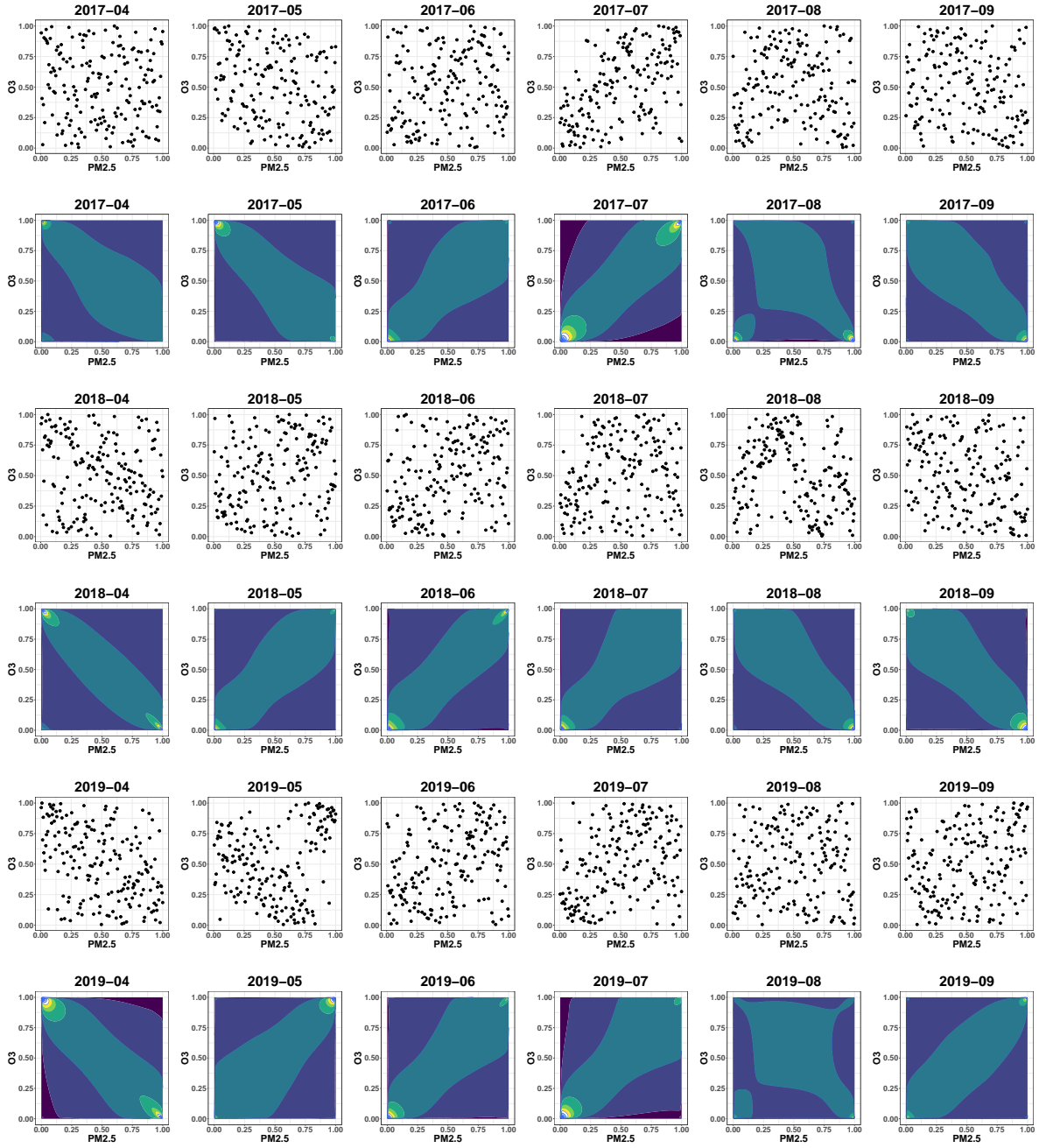


Figure 8: Observed realdata and estimated joint density from April to September 2017 (top), 2018 (middle), and 2019 (bottom). Dependence patterns tend to vary between seasons with some months exhibiting transitional regimes.